

## 样品倾转角度对透射电镜表征纳米薄膜的影响

张革<sup>1,2</sup>, 崔云<sup>1,2\*</sup>, 赵娇玲<sup>1,2\*\*</sup>, 王涛<sup>1,2</sup>, 赵元安<sup>1,2</sup><sup>1</sup>中国科学院上海光学精密机械研究所薄膜光学实验室, 上海 201800;<sup>2</sup>中国科学院上海光学精密机械研究所强激光材料重点实验室, 上海 201800

**摘要** 以沉积在Si[100]基底的Mo/Si多层膜为例,通过透射电镜(TEM)测量了多层膜在不同倾转角度下的界面结构,并提取了多层膜的周期厚度以及单周期中Mo层和Si层的厚度。结果表明:样品沿 $\alpha$ 方向倾转时,Mo层和Si层的测量厚度几乎没有变化,但界面粗糙度增大,这是由于旋转时薄膜的厚度方向始终与电子束垂直,而电子束穿过的TEM样品厚度 $Z$ 增大;样品沿 $\beta$ 方向倾转时,由于倾转时样品截面与电子束不垂直,造成伪影严重,无法区分Mo层和Si层,多层膜的测量总厚度随倾转角的增大先增大后减小。此外,提出了样品沿 $\beta$ 方向倾转后测量薄膜厚度的计算公式。对于较薄的薄膜,随着倾转角 $\beta$ 的增大,测量厚度增大;对于较厚的薄膜,随着倾转角 $\beta$ 的增大,测量厚度先增大后减小。薄膜厚度 $t_0$ 越小,沿 $\beta$ 方向倾转后测量厚度的相对误差越大。当TEM样品厚度 $Z$ 为10 nm时,沿 $\beta$ 方向倾转后测量厚度的相对误差较小。

**关键词** 透射电镜; 倾转角度; 薄膜界面; 膜层厚度

中图分类号 O4-34 文献标志码 A

DOI: 10.3788/AOS231519

## 1 引言

以13.5 nm为光源的极紫外光刻(EUVL)系统被认为是半导体工业的新一代光刻系统。由于所有材料对极紫外(EUV)辐射的吸收都很强,而且材料的折射率非常接近于1,因此EUVL光学系统全部采用反射式光学系统。为了提高光学器件的反射率,所有光学反射元件上均沉积了高反射率Mo/Si多层膜<sup>[1-2]</sup>。峰值波长为13.5 nm的Mo/Si膜堆栈中多层膜周期厚度接近7.0 nm,单层膜的厚度为3.0~4.0 nm之间,近原子精度的膜层厚度误差都会导致反射光谱的峰值波长偏移<sup>[3]</sup>。因此,准确表征Mo/Si多层膜薄膜厚度对于工艺迭代和分析来说具有重要的作用。

目前,互标法是一种比较好的提升纳米薄膜表征精度的方法<sup>[4-5]</sup>。互标法主要用到的测试方法有光谱椭圆偏振(SE)<sup>[6]</sup>、X射线反射(XRR)<sup>[7-8]</sup>、透射电镜(TEM)<sup>[7,9-13]</sup>、X射线光电子能谱(XPS)<sup>[14-16]</sup>和中能离子散射光谱(MEIS)<sup>[17]</sup>。TEM作为其中一种可视化方法,可通过晶体Si衬底的晶格常数内标来表征单晶Si wafer上沉积的纳米膜层厚度,具有较高的准确性<sup>[18]</sup>。然而,在TEM表征时若不关注Si基底的晶向或采用熔石英等非晶基底材料,则难以保证样品截面相对电子束是恰好垂直的,那么三维立体样品的二维投影成

像就会产生伪影,造成的测量误差是未知的。因此,研究样品倾转角度对TEM表征纳米薄膜的影响具有重要意义。本文以沉积在Si[100]基底的Mo/Si多层膜为例,研究了样品倾转角度对TEM表征纳米薄膜结构与厚度的影响。

## 2 实验方法

## 2.1 样品制备

利用脉冲直流溅射的方法沉积Mo/Si多层膜,本底真空优于 $8.0 \times 10^{-5}$  Pa, Ar工作压强小于0.15 Pa。在样品中心放置经过筛选的尺寸为30 mm×30 mm的prime级单晶Si wafer,其表面粗糙度优于0.25 nm。溅射装置腔室中靶材在下,将薄膜材料向上溅射至行星转动的基片上,沉积多层膜。Mo靶材尺寸为20.320 cm×8.890 cm×0.635 cm,纯度为99.95%;Si靶材尺寸为20.320 cm×8.890 cm×0.635 cm,纯度为99.999%。溅射电源为Advanced Energy公司的脉冲直流电源,阴极为美国安斯超科学公司(Angstrom Sciences, Inc)的磁控阴极,Mo靶溅射功率为150 W,掠靶速度为1.15 r/min;Si靶溅射功率为300 W,掠靶速度为0.51 r/min。

## 2.2 表征方法

使用离子减薄仪(PIPS II 695, Gatan)制备用于

收稿日期: 2023-09-05; 修回日期: 2023-10-17; 录用日期: 2023-11-01; 网络首发日期: 2023-11-17

基金项目: 国家自然科学基金(12275346)、中科院青促会会员项目(2020253)

通信作者: \*zhanggel@siom.ac.cn; \*\*jolin923@siom.ac.cn

TEM 表征的截面样品。使用 200 keV 场发射透射电子显微镜 (Talos F200X, Thermo Fisher Scientific) 表征获得多层膜的 TEM 图像和高分辨透射电镜 (HRTEM) 图像。使用双倾杆 ( $\alpha = \pm 40^\circ, \beta = \pm 30^\circ$ ) 对 TEM 截面样品进行倾转, 双倾杆倾转示意图如图 1(a) 所示, 其

中,  $\alpha$  方向为绕 X (平行于样品杆) 方向,  $\beta$  方向为绕 Y (垂直于样品杆) 方向。薄膜 TEM 截面样品放置在样品杆中的方向如图 1(b) 所示。结合图像的 profile 曲线, 得到不同倾转角度的多层膜厚度、界面粗糙度以及单个周期中的 Mo 层和 Si 层薄膜厚度。

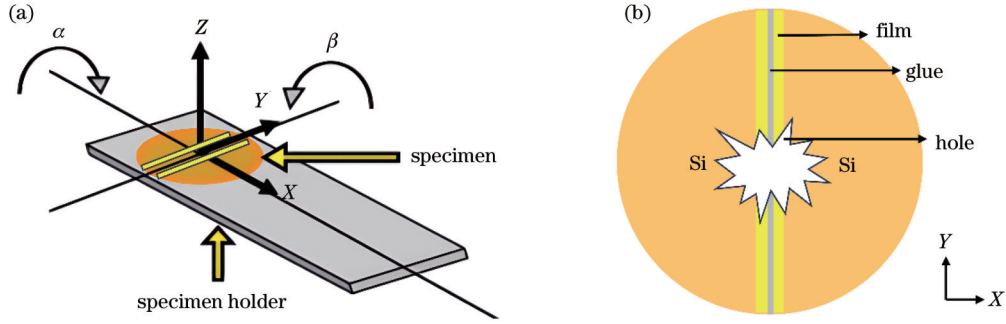


图 1 薄膜 TEM 截面样品倾转示意图。(a) 双倾杆倾转示意图; (b) 薄膜 TEM 截面样品放置在样品杆中的方向示意图  
Fig. 1 Schematic diagrams of TEM cross-section sample tilting. (a) Schematic diagram of double tilting holder; (b) orientation diagram of thin film TEM cross-section sample placed in the sample holder

### 3 结果和讨论

#### 3.1 沿 $\alpha$ 方向倾转时 Mo/Si 多层膜的厚度变化

图 2 为 40 周期的 Mo/Si 多层膜沿  $\alpha$  方向倾转后基底 Si 不同晶带轴下的 TEM 图像和 HRTEM 图像。可以看出, Mo/Si 界面始终是清晰的, 其中,  $[110]$  晶带轴下界面最为平整,  $[210]$ 、 $[310]$  晶带轴下界面较平整,

而  $[000]$  和  $[100]$  晶带轴下界面较粗糙, 这与采用  $[100]$  晶向的 Si 基底有关。图 3 为微电子工业常用的  $[100]$  晶向的单晶 Si wafer, 在 TEM 截面样品制备时沿特定方向  $[1\bar{1}0]$  切割 Si wafer, 在 TEM 表征时从  $[110]$  晶带轴观察样品, 就可以保证 Si wafer 和薄膜的截面都恰好垂直电子束, 得到准确的结果。

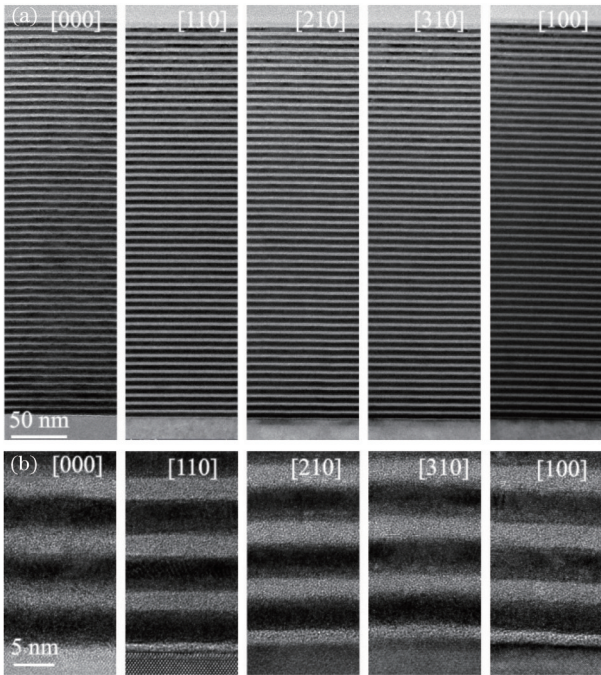


图 2 40 周期的 Mo/Si 多层膜沿  $\alpha$  方向倾转后基底 Si 不同晶带轴下的 TEM 测试结果。(a) TEM 图像; (b) HRTEM 图像  
Fig. 2 TEM results of the 40-period Mo/Si multilayer film under different crystal zone axes of the substrate Si after tilting in the  $\alpha$  direction. (a) TEM images; (b) HRTEM images

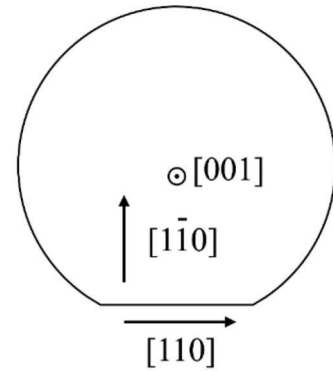


图 3  $[100]$  单晶 Si wafer 的晶体学<sup>[19]</sup>  
Fig. 3 Crystallography of  $[100]$  single-crystal Si wafer substrate<sup>[19]</sup>

利用对比度平均值法测量了以上表征薄膜的厚度, 为避免误差, 选取测量的 5 个位置的平均值作为测量结果, 结果如表 1 所示, 其中,  $D$  为 Mo/Si 多层膜周期测量厚度,  $d_{Mo}$  为单周期中 Mo 层测量厚度,  $d_{Si}$  为单周期中 Si 层测量厚度。样品沿  $\alpha$  方向倾转时, 单个周期中的 Mo 层和 Si 层薄膜厚度几乎没有变化, 约有 0.1 nm 的误差, 40 周期的薄膜总厚度最大误差也仅有 1.3 nm。样品沿  $\alpha$  方向倾转的示意图如图 4 所示, 其中,  $t_0$  为薄膜的真实厚度,  $t_\alpha$  为沿  $\alpha$  方向倾转后的薄膜厚度。沿  $\alpha$  方向倾转时, 薄膜的厚度方向始终与电子束方向 ( $Z$  轴) 垂直, 所以厚度保持与  $[110]$  晶带轴时的厚

度一致,但是粗糙度增大。与[110]晶带轴不同的是,沿 $\alpha$ 方向倾转时,电子束穿过的 TEM 样品厚度 $Z$ 增大

了,这意味着界面层处有更多的投影叠加,因此,界面粗糙度会增大。

表 1 40 周期的 Mo/Si 多层膜沿 $\alpha$ 方向倾转后的厚度变化

Table 1 Thickness change of the 40-period Mo/Si multilayer film after tilting in the  $\alpha$  direction

Crystal orientation	Tilt ( $\alpha, \beta$ )	Total thickness /nm	$D$ /nm	dMo /nm	dSi /nm
Non-tilt	(0,0)	356.8	7.043	4.096	3.056
[110]	(-4.33°, -1.57°)	355.7	7.047	4.054	2.983
[210]	(13.99°, -2.47°)	356.4	7.016	3.967	3.038
[310]	(22.27°, -3.15°)	356.6	7.053	3.989	3.063
[100]	(40.44°, -4.94°)	357.0	7.053	4.082	2.943

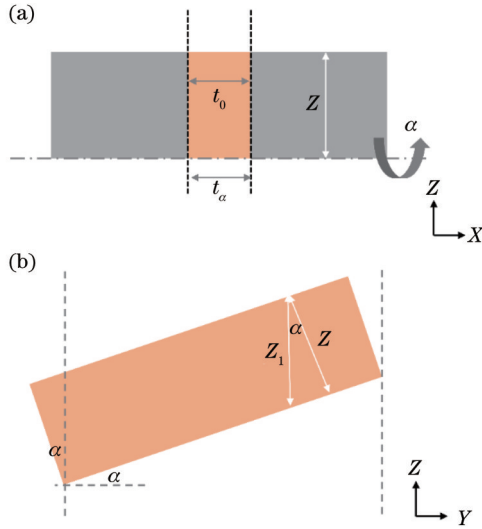


图 4 TEM 样品沿 $\alpha$ 方向倾转的示意图。(a)XZ 面;(b)YZ 面  
Fig. 4 Schematic diagrams of TEM sample tilting in the  $\alpha$  direction. (a) XZ plan; (b) YZ plan

### 3.2 沿 $\beta$ 方向倾转时 Mo/Si 多层膜的厚度变化

图 5 为 40 周期的 Mo/Si 多层膜沿 $\beta$ 方向倾转后 Si 基底不同晶带轴下的 TEM 图像,可以看出,[332]和近[111]晶带轴下,Mo 层和 Si 层交错叠加,膜层界面难以区分。表 2 为 40 周期的 Mo/Si 多层膜沿 $\beta$ 方向倾转后的厚度变化,可以看出,沿 $\beta$ 方向倾转,Mo/Si 多层膜的厚度逐渐减小。

为了进一步分析沿 $\beta$ 方向倾转对 Mo/Si 多层膜的影响,测量了沿 $\beta$ 方向每倾转 $10^\circ$ 多层膜的厚度,结果如图 6 所示。可以看出:当倾转角度为 $10^\circ$ 左右时,厚度增大了 1 nm;当倾转角度达到 $20^\circ$ 时,厚度减小了约 3 nm;当倾转角度达到 $30^\circ$ 时,厚度减小约 10 nm,给纳米薄膜的测量结果带来了巨大偏差。

样品沿 $\beta$ 方向倾转的示意图如图 7 所示,样品截面与电子束方向( $Z$ 轴方向)不垂直,在投影成像时产生伪影。样品沿 $\beta$ 方向倾转后的薄膜厚度 $t_\beta$ 为

$$t_\beta = t_0 \cos \beta + Z \sin \beta, \quad (1)$$

式中: $t_0$ 为薄膜的真实厚度; $\beta$ 为沿 $\beta$ 方向的倾转角度; $Z$ 为 TEM 样品的厚度。离子减薄的 TEM 截面样品厚度 $Z$ 一般在 10~100 nm,取 $Z=50$  nm,对 $t_0=5$ 、20、

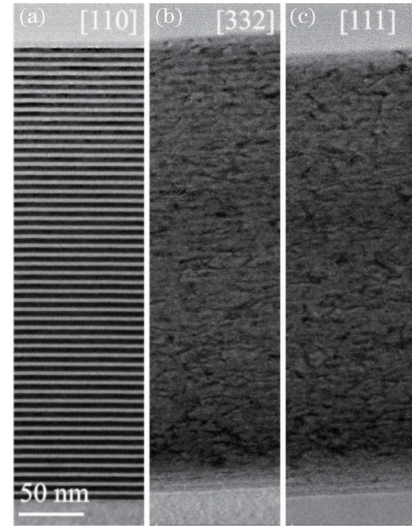


图 5 40 周期的 Mo/Si 多层膜沿 $\beta$ 方向倾转后 Si 基底不同晶带轴下的 TEM 图像

Fig. 5 TEM images of the 40-period Mo/Si multilayer film under different crystal zone axes of the substrate Si after tilting in the  $\beta$  direction

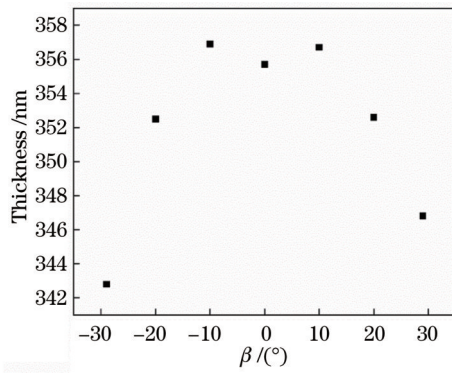
表 2 40 周期的 Mo/Si 多层膜沿 $\beta$ 方向倾转后的厚度变化  
Table 2 Thickness change of the 40-period Mo/Si multilayer film after tilting in the  $\beta$  direction

Crystal orientation	Tilt ( $\alpha, \beta$ )	Total thickness /nm
Non-tilt	(0,0)	356.8
[332]	(-1.75°, -21.67°)	355.6
[111]	(-0.06°, -29.81°)	346.8

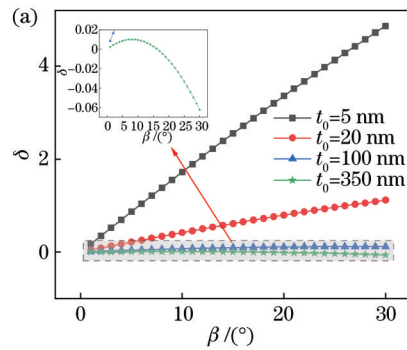
100、350 nm 这 4 种不同厚度的薄膜进行计算,其中,相对误差 $\delta$ 表示为

$$\delta = (t_\beta - t_0) / t_0. \quad (2)$$

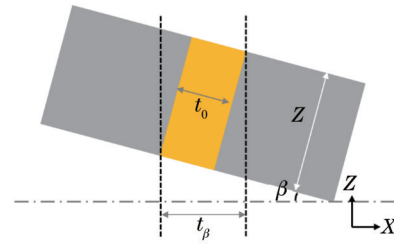
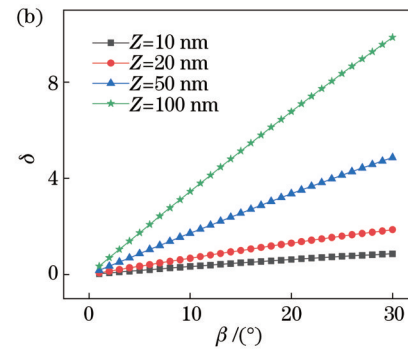
计算结果如图 8(a)所示。可以看出:5 nm 的薄膜在倾转后厚度甚至是原来的几倍。此结果与 Kang 等<sup>[20]</sup>在利用能量色散 X 射线谱测量纳米薄膜厚度的新方法中的研究结果一致。20 nm 的薄膜在倾转后厚度增大明显,但未成倍数增大。350 nm 的薄膜在倾转后厚度先增大再减小,相对误差小于 10%,与样品其他测试结果趋势一致。这表明,薄膜厚度 $t_0$ 越小,倾转角

图 6 40 周期的 Mo/Si 多层膜沿  $\beta$  方向倾转后的厚度变化Fig. 6 Thickness change of the 40-period Mo/Si multilayer film after tilting in the  $\beta$  direction

$\beta$  对测量结果的影响越大。取  $t_0=5$  nm,  $Z=10、20、50、$

图 8 相对误差  $\delta$  随倾转角度  $\beta$  变化的计算结果。(a)  $Z=50$  nm, 不同  $t_0$  的薄膜;Fig. 8 Calculation results of relative error  $\delta$  varies with the tilting angle  $\beta$ . (a) Thin films with  $Z=50$  nm and different  $t_0$ ; (b) thin films with  $t_0=5$  nm and different  $Z$ 

100 nm 进行计算,结果如图 8(b)所示。可以看出, $Z=10$  nm 时,相对误差曲线相对平滑,沿  $\beta$  方向倾转后测量厚度的相对误差较小。这说明在制备 TEM 截面样品时,应尽可能地把样品减薄。

图 7 TEM 样品沿  $\beta$  方向倾转的示意图Fig. 7 Schematic diagram of TEM sample tilting in the  $\beta$  direction

## 4 结 论

TEM 样品沿  $\alpha$  方向倾转对测量的薄膜厚度几乎没有影响,但膜层的粗糙度增大,这是因为倾转时薄膜的厚度方向始终与电子束垂直,而 TEM 样品厚度  $Z$  增大。TEM 样品沿  $\beta$  方向倾转时,对于较薄的薄膜,随着倾转角的增大测量厚度增大;对于较厚的薄膜,随着倾转角的增大测量厚度先增大后减小;薄膜越薄,倾转后厚度的相对误差越大,这是由倾转时样品截面与电子束不垂直造成的伪影导致的;TEM 样品厚度  $Z=10$  nm 时,沿  $\beta$  方向倾转后测量厚度的相对误差较小。因此,通过 TEM 表征纳米薄膜结构与厚度时,应从制样开始沿特定方向  $[1\bar{1}0]$  切割 Si wafer,再从  $[110]$  晶带轴观察样品,这样就可以保证 Si wafer 和薄膜的截面都恰好与电子束垂直。在 TEM 样品较薄的区域拍照分析得出,采用此方法得到的结果更加准确。

### 参 考 文 献

- [1] Louis E, Yakshin A E, Tsarfati T, et al. Nanometer interface and materials control for multilayer EUV-optical applications[J]. Progress in Surface Science, 2011, 86(11/12): 255-294.
- [2] Wagner C, Harned N. EUV lithography: lithography gets

extreme[J]. Nature Photonics, 2010, 4(1): 24-26.

- [3] 喻波. 极紫外多层膜厚梯度控制及抗热损伤研究[D]. 长春: 中国科学院长春光学精密机械与物理研究所, 2016: 3-6. Yu B. Study on film thickness gradient control and thermal damage resistance of extreme ultraviolet multilayer films[D]. Changchun: Changchun Institute of Optics, Fine Mechanics and Physics, Chinese Academy of Sciences, 2016: 3-6.
- [4] Kim K J. Review on the thickness measurement of ultrathin oxide films by mutual calibration method[J]. Surface and Interface Analysis, 2022, 54(4): 405-416.
- [5] 李超逸, 陶保全, 郭祥帅, 等. 极紫外多层膜技术的研究进展[J]. 量子光学学报, 2020, 26(4): 397-408. Li C Y, Tao B Q, Guo X S, et al. Research progress on extreme ultraviolet multilayer techniques[J]. Journal of Quantum Optics, 2020, 26(4): 397-408.
- [6] 吴曼玉, 黄水平. Zr 基薄膜金属玻璃的制备及其光学常数测定[J]. 光子学报, 2020, 49(10): 1031001. Wu M Y, Huang S P. Preparation of Zr-based thin film metallic glass and determination of its optical constant[J]. Acta Photonica Sinica, 2020, 49(10): 1031001.
- [7] Chassé T, Neumann H, Ocker B, et al. Mo/Si multilayers for EUV lithography by ion beam sputter deposition[J]. Vacuum, 2003, 71(3): 407-415.
- [8] Valkovskiy G A, Baidakova M V, Brunkov P N, et al. Integrated characterization of multilayer periodic systems with nanosized layers as applied to Mo/Si structures[J]. Physics of the Solid State, 2013, 55(3): 648-658.
- [9] Jiang H, Michette A, Pfauntsch S, et al. Determination of the evolution of layer thickness errors and interfacial imperfections in

- ultrathin sputtered Cr/C multilayers using high-resolution transmission electron microscopy[J]. *Optics Express*, 2011, 19(12): 11815-11824.
- [10] Nedelcu I, van de Kruijs R W E, Yakshin A E, et al. Thermally enhanced interdiffusion in Mo/Si multilayers[J]. *Journal of Applied Physics*, 2008, 103(8): 083549.
- [11] Yulin S, Feigl T, Kuhlmann T, et al. Interlayer transition zones in Mo/Si superlattices[J]. *Journal of Applied Physics*, 2002, 92(3): 1216-1220.
- [12] Yu B, Jin C S, Yao S, et al. Low-stress and high-reflectance Mo/Si multilayers for extreme ultraviolet lithography by magnetron sputtering deposition with bias assistance[J]. *Applied Optics*, 2017, 56(26): 7462-7468.
- [13] Meltchakov E, Vidal V, Faik H, et al. Performance of multilayer coatings in relationship to microstructure of metal layers. Characterization and optical properties of Mo/Si multilayers in extreme ultra-violet and X-ray ranges[J]. *Journal of Physics: Condensed Matter*, 2006, 18(13): 3355-3365.
- [14] Kim K J, Jang J S, Lee J H, et al. Determination of the absolute thickness of ultrathin Al<sub>2</sub>O<sub>3</sub> overlayers on Si (100) substrate[J]. *Analytical Chemistry*, 2009, 81(20): 8519-8522.
- [15] Kim K J, Lee S M, Jang J S, et al. Thickness measurement of a thin hetero-oxide film with an interfacial oxide layer by X-ray photoelectron spectroscopy[J]. *Applied Surface Science*, 2012, 258(8): 3552-3556.
- [16] Kim K J, Kim T G, Kwon J H, et al. Traceable thickness measurement of ultra-thin HfO<sub>2</sub> films by medium-energy ion scattering spectroscopy[J]. *Metrologia*, 2020, 57(2): 025001.
- [17] Shin J Y, Min W J, Chang H S, et al. Thickness measurement of ultra-thin TiO<sub>2</sub> films by mutual calibration method[J]. *Applied Science and Convergence Technology*, 2020, 29(3): 50-54.
- [18] Höche T. Cross-sectional high-resolution transmission electron microscopy at Mo/Si multilayer stacks[J]. *International Journal of Materials Research*, 2022, 97(7): 1046-1050.
- [19] Bravman J C, Sinclair R. The preparation of cross-section specimens for transmission electron microscopy[J]. *Journal of Electron Microscopy Technique*, 1984, 1(1): 53-61.
- [20] Kang M C, Oh J S, Song K Y, et al. Novel method of measuring the thickness of nanoscale films using energy dispersive X-ray spectroscopy line scan profiles[J]. *Advanced Materials Interfaces*, 2022, 9(7): 2101489.

## Effect of Sample Tilting Angle on the Characterization of Nanofilms by Transmission Electron Microscopy

Zhang Ge<sup>1,2</sup>, Cui Yun<sup>1,2\*</sup>, Zhao Jiaoling<sup>1,2\*\*</sup>, Wang Tao<sup>1,2</sup>, Zhao Yuan'an<sup>1,2</sup>

<sup>1</sup>Laboratory of Thin Film Optics, Shanghai Institute of Optics and Fine Mechanics, Chinese Academy of Sciences, Shanghai 201800, China;

<sup>2</sup>Key Laboratory of Materials for High Power Laser, Shanghai Institute of Optics and Fine Mechanics, Chinese Academy of Sciences, Shanghai 201800, China

### Abstract

**Objective** Accurate characterization of Mo/Si multilayer film thickness is important for process iteration and analysis. As one of the visualization methods, transmission electron microscopy (TEM) can characterize the thickness of nanofilm deposited on a single crystal Si wafer. It can be calibrated internally through the Si substrate lattice parameters, which is very accurate. However, if we do not pay attention to the crystal orientation of the Si substrate during TEM characterization or we use amorphous substrate materials such as fused quartz, it is difficult to ensure that the cross-section of the sample is exactly perpendicular to the electron beam. As a result, the two-dimensional projection imaging of three-dimensional samples produces artifacts, resulting in unknown measurement errors. Therefore, it is of great significance to study the influence of sample tilting angle on the TEM characterization of nanofilms.

**Methods** Mo/Si multilayer films are deposited by pulsed direct current sputtering. Cross-section samples for TEM characterization are prepared by ion milling. TEM images and high-resolution TEM images of the multilayer films are obtained by TEM. The TEM cross-section samples are tilted in  $\alpha$  and  $\beta$  directions by a double tilting holder. Combined with the profile curves of the images, we obtain the thickness of the multilayer film at different tilting angles, the roughness of the interface, and the thickness of the Mo and Si layers in a single period.

**Results and Discussions** As the Mo/Si multilayer film sample tilting in the  $\alpha$  direction, the thickness direction of the film is always perpendicular to the electron beam direction ( $Z$  axis), so the thickness does not change. The roughness increases, because the thickness  $Z$  of the TEM sample which the electron beam passes increases as tilting in the  $\alpha$  direction. It implies more projective superposition at the interface layer (Fig. 4). As tilting in the  $\beta$  direction, the sample cross-section is not perpendicular to the electron beam direction ( $Z$  axis), resulting in artifacts during projection imaging and a large deviation (Fig. 7). A formula for measuring the thickness of thin films after the sample tilting in the  $\beta$  direction is proposed. For thin films, the measured thickness increases with the increase of the tilting angle  $\beta$ . For thicker films, the measured thickness first increases and then decreases with the increase of tilting angle  $\beta$ . A thinner film thickness  $t_0$  causes

a greater relative error of the measured film thickness after tilting in the  $\beta$  direction (Fig. 8).

**Conclusions** As the sample tilting in the  $\alpha$  direction, the measured thickness of the Mo and Si layers is almost unchanged while the interface roughness increases. This is because the thickness direction of the film is always perpendicular to the electron beam during rotation, and the thickness  $Z$  of the TEM sample which the electron beam through increases. The artifacts caused by the sample cross-section are not perpendicular to the electron beam during tilting, which is too severe to distinguish the Mo layer and the Si layer. The measured total thickness of the multilayer film first increases and then decreases with the increasing tilting angle. The formula for calculating the thickness of the film after the sample tilting in the  $\beta$  direction is presented. For thin films, the measured thickness increases with the increasing tilting angle. For thicker films, the measured thickness first increases and then decreases with the increasing tilting angle. As the film thickness  $t_0$  becomes thinner, the relative error is greater after tilting in the  $\beta$  direction. When the TEM sample thickness  $Z$  is 10 nm, the relative error of measuring thickness is small after tilting in the  $\beta$  direction. Therefore, when characterizing the structure and thickness of nanofilm by TEM, Si wafers should be cut in a specific direction  $[1\bar{1}0]$  from the beginning of sample preparation. Then samples should be observed from the crystal band axis  $[110]$ . Only in this way, it can ensure that the cross sections of Si wafers and films are exactly perpendicular to the electron beam. Photograph and analysis in the thin area of the TEM sample show that the result obtained by this method is more accurate.

**Key words** transmission electron microscopy; tilting angle; film interface; film thickness